Electric field control of multiferroic domain wall motion

Hong-Bo Chen, Ye-Hua Liu, and You-Quan Li

Citation: Journal of Applied Physics **115**, 133913 (2014); doi: 10.1063/1.4870711
View online: http://dx.doi.org/10.1063/1.4870711
View Table of Contents: http://scitation.aip.org/content/aip/journal/jap/115/13?ver=pdfcov
Published by the AIP Publishing

Electric field control of multiferroic domain wall motion

Hong-Bo Chen, Ye-Hua Liu, and You-Quan Li
Zhejiang Institute of Modern Physics and Department of Physics, Zhejiang University, Hangzhou 310027, People's Republic of China

(Received 10 March 2014; accepted 26 March 2014; published online 4 April 2014)

The dynamics of a multiferroic domain wall in which an electric field can couple to the magnetization via inhomogeneous magnetoelectric interaction is investigated by the collective-coordinate framework. We show how the electric field is capable of delaying the onset of the Walker breakdown of the domain wall motion, leading to a significant enhancement of the maximum wall velocity. Moreover, we show that in the stationary regime the chirality of the domain wall can be efficiently reversed when the electric field is applied along the direction of the magnetic field. These characteristics suggest that the multiferroic domain wall may provide a new prospective means to design faster and low-power-consumption domain wall devices. © *2014 AIP Publishing LLC*.
[http://dx.doi.org/10.1063/1.4870711]

I. INTRODUCTION

Manipulation of magnetic properties by an external electric field has long been a big challenge in the quest for novel spintronic devices. In conventional ferroelectric or ferromagnetic materials, the controlled motion of ferroic domain walls (DWs) is essential to achieve the desired functionalities.[1,2] Usually, the motion of DW in magnetic materials are driven by a magnetic field[3–5] or spin-polarized current.[6,7] A key concept in the context of DW motion is the so-called Walker breakdown,[3] which distinguishes the two regimes with high- and low-mobility and sets a limit to the DW velocity. To achieve fast and efficient control of DW motion, various attempts have been made to prevent this breakdown process, such as applying a transverse field[8–11] or considering a perpendicular magnetic anisotropy,[12–14] and the spin-orbit coupling effect.[15–19] In this context, a way to manipulate the dynamics of the DWs by an electric field, which is critical for developing low-power-consumption spintronic devices, would be extremely appealing. Recently, it has been shown that modulating the magnetic anisotropy by an applied electric field is possible,[20,21] and thus will allow for the electric field control of DW dynamics in ultrathin metallic ferromagnets.[22–28] Nevertheless, the search for alternative schemes allowing fast and energy-efficient DW propagation is of great relevance in advanced spintronics research.

Multiferroic materials,[29] which exhibit simultaneously ferroelectric and magnetic orders, may provide a promising arena to realize electric control of magnetization and even for DW motion. Multiferroics display a particularly rich variety of magnetoelectric (ME) cross-coupling effects. An intriguing scenario of ME coupling is that spiral spin orders can by themselves produce electric polarization, which is called the spin-current mechanism,[30–33] or equivalently the *inhomogeneous magnetoelectric interaction*.[34] Therefore, a nonzero electric polarization can be induced not only just in bulk but also within local magnetic textures, like magnetic DWs and vortices. The possibility of such a magnetoelectricity in ferromagnetic Néel walls has been anticipated theoretically[34,35] and recently demonstrated experimentally.[36,37] Especially, this ME coupling also enables the electric field couple to the magnetization with its spatial gradients, which necessarily presents in metallic as well as insulating ferromagnets.[38] The influence of this coupling on the spin waves of the multiferroics has recently been explored in Ref. 39. However, the relevance of the electric field to the motion of a multiferroic DW, even though it is crucial to future ME multiferroic devices based on DW control, still remains unclear.

In this paper, we identify the dynamical nature of a prototypical type of multiferroic DW, that is, a magnetic DW simultaneously displaying an electric polarization. This is a good basis for studying the dynamical properties of the multiferroic DWs in which the electric field can couple to the magnetization via the inhomogeneous magnetoelectric interaction. We derive the equations of motion for electric field controlled DW dynamics in such a multiferroic DW. We report two main findings. The first one is that the magnetic DW velocity can be considerably enhanced due to the delay of the occurrence of Walker breakdown by an applied electric field. This electric-field-modulated higher DW speed implies faster device operation, which is one of the main aim of the conventional DW device applications. The second finding is that the electric field can be used to control the switching of the DW chirality. This control of the chirality could provide an additional degree of freedom, which can be useful in future magnetoelectric logic devices.

The paper is organized as follows: In Sec. II, we present the model for a multiferroic DW. We obtain the equations of motion for the multiferroic DW dynamics using the collective coordinate description. In Sec. III, we discuss how the electric field influences the DW velocity and the chirality switching. At the end, in Sec. IV, we present a brief summary of the results obtained in this work.

II. THEORETICAL MODEL

The system under consideration is schematically depicted in Fig. 1. We will focus on a case of one-dimensional

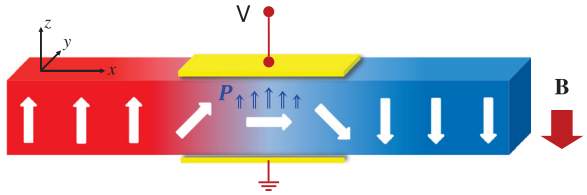

FIG. 1. Schematic of the one-dimensional multiferroic DW structure consisting of a Néel-type magnetic DW which induces an electric polarization (blue arrows) within the DW. A voltage is applied along the z direction, while the external magnetic field $\mathbf{B}$ is kept in $-\hat{z}$ direction. The white broad arrows denote the local spins in the wall.

insulating Néel-type DW when magnetic easy (hard) axis is taken to be along the $\hat{z}$ ($\hat{y}$) direction with a voltage applied along the z direction. The theoretical model we employ consists of three distinct contributions

$$\mathcal{H} = \mathcal{H}_S + \mathcal{H}_Z + \mathcal{H}_E. \tag{1}$$

The first contribution $\mathcal{H}_S$ describes the Hamiltonian of local spins in a magnetic DW, with an easy axis and a hard axis, chosen as $\hat{z}$ and $\hat{y}$ directions, respectively. In the continuum limit, this Hamiltonian takes the form[40]

$$\mathcal{H}_S = \int \frac{d^3x}{a^3}\left[\frac{J}{2}(\nabla \mathbf{S})^2 - \frac{K}{2}(S_z)^2 + \frac{K_\perp}{2}(S_y)^2\right]. \tag{2}$$

Here, $\mathbf{S}$ is the local spin vector, a is the lattice constant, J is the exchange coupling between local spins, while K and $K_\perp$ are anisotropy energies associated with the easy and hard axes of the spins, respectively. Here, we consider a homogeneous system, i.e., a system without pinning potential. In terms of spherical coordinates (θ, ϕ), the energy functional in Eq. (2) has a stationary DW as a classical solution

$$\theta(x) = 2\arctan[e^{(x-X)/\lambda_{DW}}], \quad \phi(x) = \phi_0, \tag{3}$$

which gives the x-dependent spin configuration

$$\mathbf{S} = S(\sin\theta\cos\phi_0, \sin\theta\sin\phi_0, \cos\theta), \tag{4}$$

with S is the magnitude of spin. In Eq. (3), X is the position of the DW center, $\lambda_{DW} = \sqrt{J/K}$ is the DW width. ϕ_0 is the tilting angle between spins at the DW center and the easy plane, which is spatially homogeneous. In particular, if $\phi_0 = 0$ or π, the domain wall considered above is called pure Néel wall (as shown in Fig. 1) with opposite chirality: clockwise (CW) or counterclockwise (CCW), respectively, while if $\phi_0 = \pm\pi/2$ the wall becomes a pure Bloch wall. Such a description of the DW assumes its rigidity, that is, the DW can only move or rotate.

The second ingredient of our model is the Zeeman energy, which is given by

$$\mathcal{H}_Z = -\int d^3x \mathbf{M}\cdot\mathbf{B}, \tag{5}$$

where $\mathbf{M} = -g\frac{\hbar}{a^3}\mathbf{S}$ is the magnetic moment per unit volume, $g(>0)$ is the gyromagnetic ratio, and $\mathbf{B}$ is a uniform external magnetic field pointing along the negative z direction, i.e., $\mathbf{B} = -B\hat{z}$, $B > 0$.

The third contribution $\mathcal{H}_E$ models the coupling between the electric field and the spin degrees of freedom of the multiferroic DW. According to the inhomogeneous magnetoelectric interaction,[34] we take the following form:

$$\mathcal{H}_E = -\mathbf{E}\cdot\mathbf{P}, \tag{6}$$

with the electric polarization $\mathbf{P}$ induced within the DW given as[34]

$$\mathbf{P} = \gamma_0 \int \frac{d^3x}{a^3}[\mathbf{S}(\nabla\cdot\mathbf{S}) - (\mathbf{S}\cdot\nabla)\mathbf{S}], \tag{7}$$

where γ_0 is the magnetoelectric coupling coefficient. One can learn immediately from Eq. (7) that inhomogeneous magnetoelectric interaction induces electric polarization $\mathbf{P}$ within the Néel wall so that it is actually multiferroic.

To study the dynamics of a rigid planar DW, we employ a well-known collective coordinate description.[40] In this approach, the position X and angle ϕ_0 in Eq. (3) of the wall is regarded as time-dependent collective coordinates $\{X(t), \phi_0(t)\}$. The chirality of the DW is determined by the tilt angle $\phi_0(t)$. The domain wall is described by a Lagrangian of local spins given by

$$\mathcal{L} = \int \frac{d^3x}{a^3}\hbar S\dot{\phi}_0(\cos\theta - 1) - \mathcal{H}. \tag{8}$$

The first term represents the spin Berry phase. Inserting the DW ansatz (Eq. (3)) into Eq. (8) and integrating the space coordinate, the DW Lagrangian in terms of $X(t)$ and $\phi_0(t)$ can be written as

$$\mathcal{L} = -\frac{\hbar NS}{\lambda_{DW}}\left(X\dot{\phi} + v_\perp \sin^2\phi_0 - gBX - \gamma E\cos\phi_0\right). \tag{9}$$

Here, $N = 2A\lambda_{DW}/a^3$ is the number of spins in the wall region, with A being the cross-sectional area of the system, $v_\perp = \lambda_{DW}K_\perp S/2\hbar$, and $\gamma = \pi S\gamma_0/2\hbar$. To derive the equations of motion of a DW, one further needs to introduce the dissipation function $\mathcal{W}$ to incorporate the Gilbert damping, which is written as[40]

$$\mathcal{W} = \int \frac{d^3x}{a^3}\frac{\hbar\alpha}{2S}\dot{\mathbf{S}}^2 = \frac{\alpha\hbar NS}{2}\left[\left(\dot{X}/\lambda_{DW}\right)^2 + \dot{\phi}_0^2\right], \tag{10}$$

where α is the Gilbert damping parameter. We then utilize the generalized Euler-Lagrangian equation[40]

$$\frac{d}{dt}\frac{\delta\mathcal{L}}{\delta\dot{q}} - \frac{\delta\mathcal{L}}{\delta q} = -\frac{\delta\mathcal{W}}{\delta\dot{q}}, \tag{11}$$

where q represents $X(t)$ and $\phi_0(t)$ and the last term describes the energy dissipated. The equations of motion for the collective coordinates, derived from the Eqs. (9)–(11), are given as follows:

$$\frac{\dot{X}}{\lambda_{DW}} - \alpha\dot{\phi}_0 = \frac{v_\perp}{\lambda_{DW}}\sin 2\phi_0 + \frac{\gamma E}{\lambda_{DW}}\sin\phi_0, \tag{12a}$$

$$\dot{\phi}_0 + \alpha\frac{\dot{X}}{\lambda_{DW}} = gB. \tag{12b}$$

These equations provide a basic description of the multiferroic DW dynamics under the magnetic and electric fields. Thus, the application of the electric field on the DW introduces an additional spin torque proportional to $\sin\phi_0$ into the equations of motion. This new term will act as a chirality stabilizer, influencing significantly the DW dynamics. In what follows, we solve Eqs. (12) numerically and calculate the values for X and ϕ_0 after a sufficiently long time. The average terminal velocity of the DW is defined as $v_{DW} = \langle \dot{X} \rangle$, where the angular brackets refer to a long-time average. To do the numerical simulation, we take a fixed value for the Gilbert damping parameter $\alpha = 0.02$. The initial DW tilt angle is set to $\phi_{0i} = \phi_0(t = 0) = 0$ throughout, so the initial chirality of the DW is clockwise.

III. RESULTS AND DISCUSSION

A. Electric field mediated DW velocity

Let us discuss, how the electric field affects the field-driven DW motion based on the equations of motion we derived previously. The numerical simulation results of Eqs. (12) are presented in Figs. 2–4. It is important to note that when the electric field is switched off, the equations of motion in Eqs. (12) are reduced to those of a DW purely driven by a magnetic field, whose behaviours are well known.[3,4,40] In that case, the DW motion is characterized by the existence of two dynamic regimes, separated by a threshold field called Walker field.[3] That is, for an external field smaller than the Walker field $B_W = \alpha K_\perp S/2g\hbar$, the DW moves with a constant velocity which increases linearly with the external magnetic field up to B_W. In this regime, the DW chirality which describes the sense of rotation of the spins in the wall is preserved during the motion. For fields $B > B_W$, the Walker breakdown occurs and the DW undergoes oscillatory motion, which makes the DW velocity decrease rapidly. Such a behaviour was originally predicted by Schryer and Walker[3] and was observed experimentally, for example, by Beach *et al.*[5]

We first show in Fig. 2 the time-averaged precession velocity $\langle \dot{\phi}_0 \rangle$, as a function of magnetic field B for various values of electric fields applied along $+\hat{z}$ direction. We find that $\langle \dot{\phi}_0 \rangle = 0$ up to a threshold applied field, even when the external electric field is switched on. This zero precession velocity means that the wall angle ϕ_0 tilts out of the plane until it reaches a certain angle. From then on, it no longer changes. In the regime, where $\langle \dot{\phi}_0 \rangle = 0$ the wall moves at a constant velocity. As $\langle \dot{\phi}_0 \rangle$ becomes finite, the wall tilt angle ϕ_0 starts precessing, causing an oscillatory motion that slows down the domain wall. In Fig. 2, we clearly see that the zero $\langle \dot{\phi}_0 \rangle$ regime (stationary regime) is significantly extended by the application of an electric field.

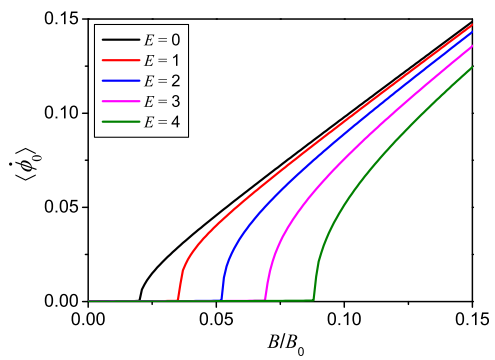

FIG. 2. The behavior of the time-averaged precession velocity $\langle \dot{\phi}_0 \rangle$ as a function of magnetic field B at several applied electric field E. $\langle \dot{\phi}_0 \rangle$ is given in units of $K_\perp S/2\hbar$, the electric field E is given in units of $E_0 = v_\perp/\gamma$, and units $B_0 = K_\perp S/2g\hbar$. The regime with $\langle \dot{\phi}_0 \rangle = 0$ represents the stationary regime of the DW motion.

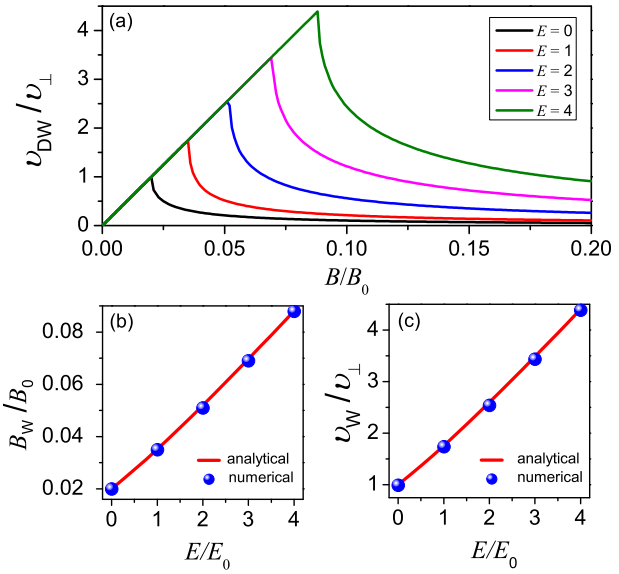

FIG. 3. (a) The velocity of the DW v_{DW} as a function of B under the application of various E applied along the $+\hat{z}$ direction. E is given in units of $E_0 = v_\perp/\gamma$. (b) and (c) are the dependence of the Walker field B_W and the Walker velocity v_W with the electric field, respectively. Both show a quasi-linear increase with E.

Figure 3(a) shows the time-averaged DW velocity v_{DW} as a function of B for several applied electric fields. When the electric field is switched on, the v_{DW} (B) curves show similar behavior to that of the conventional magnetic field driven model. For each applied E, v_{DW} reaches a maximum velocity, namely, Walker velocity (v_W). The corresponding threshold magnetic field is Walker field (B_W), and above B_W the v_{DW} drops abruptly. More specifically, the Walker field B_W increases with E and there is no change of DW mobility. It seems that the presence of an electric field surely acts as a chirality stabilizer and plays a pivotal role to delay the onset of the Walker breakdown and allows for higher attainable DW velocities. Figures 3(b) and 3(c) summarize the increase of both the Walker field B_W and the Walker velocity v_W with the magnitude of E. It is clearly shown that both B_W and v_W exhibit a nearly linear behavior, so we have an scenario where the maximum velocity of the wall is substantially enhanced by the application of an electric field.

To elucidate the role of the electric field in the suppression of Walker breakdown, we further examine analytically the DW dynamics for B smaller than B_W, since in such a stationary regime $\partial\phi_0/\partial t = 0$ as $t \to \infty$. From Eqs. (12), we obtain

$$\frac{B}{\alpha B_0} = \sin 2\phi_0 + \Delta \sin \phi_0, \tag{13}$$

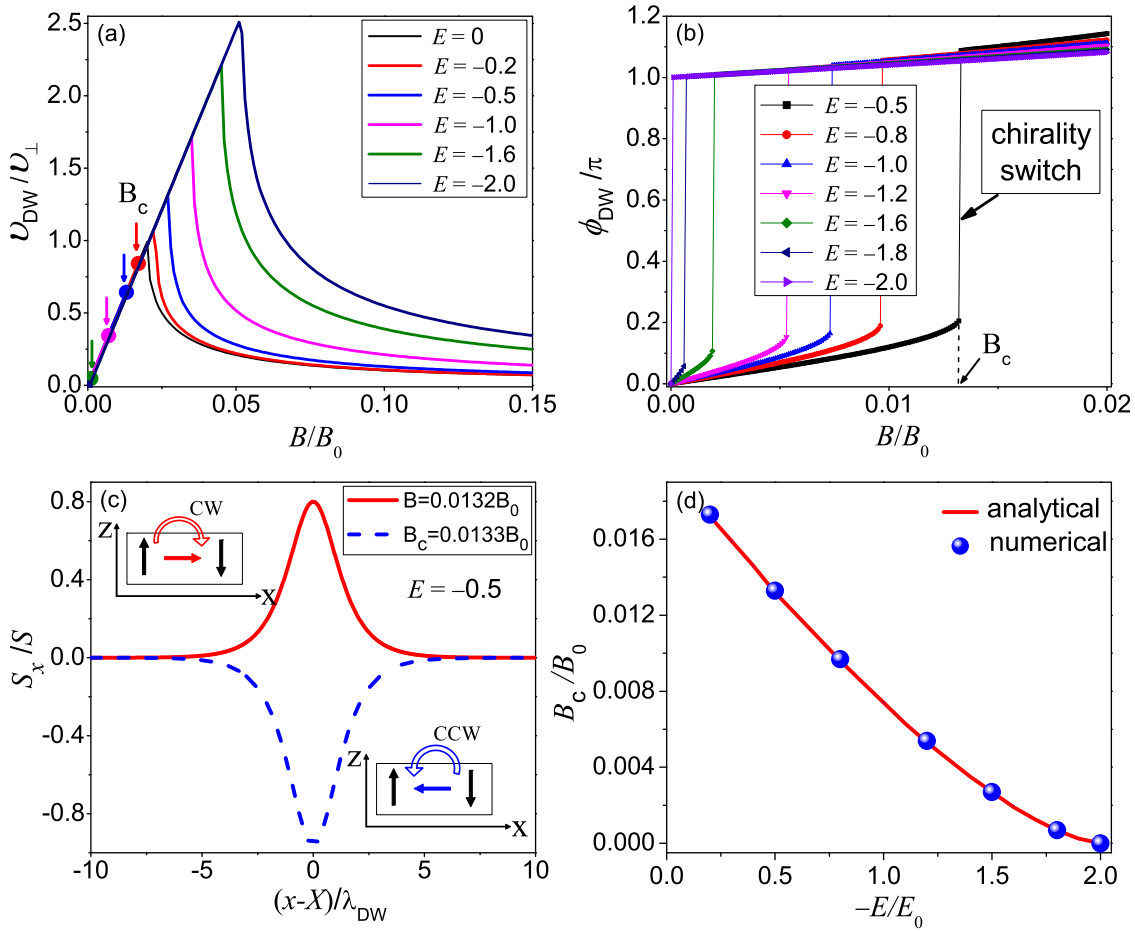

FIG. 4. (a) B dependence of the DW velocity v_{DW} for several choices of E applied along the $-\hat{z}$ axis. The color dots mark the critical fields B_{c} indicating the chirality switching for each case. (b) The terminal DW tilt angle ϕ_{DW} as a function of B. The sudden jumps of ϕ_{DW} denote the chirality switching occurring, from CW to CCW. (c) Component of the spin along the x-axis (spin modulation direction) at the DW center. Below B_c, $S_x > 0$ (red solid line) means CW chirality; and above B_c, $S_x < 0$ (blue dashed line) means CCW chirality. The applied $E = -0.5E_0$. (d) The dependence of B_{c} with the field strength $|E|$.

where $B_0 = K_\perp S/2g\hbar$ and $\Delta = E/E_0$, with $E_0 = v_\perp/\gamma$. As long as this equation is satisfied, the DW will propagate without oscillatory motion. The Walker field B_{W} is determined from the maximum of the r.h.s. of Eq. (13). Equation (13) shows that B_{W} depends not only on the sign of Δ (or E) but also on the initial tilt angle $\phi_{0i}(=\phi_0(t=0))$ (either 0 or π). The Walker field B_{W} is found to be associated with the tilt angle $\phi_{0\mathrm{W}} = \arccos[(-\Delta + \sqrt{\Delta^2+32})/8]$. Then, we can obtain the Walker field as $B_{\mathrm{W}}(\phi_{0i}=0, E>0) = B_{\mathrm{W1}}$ with

$$B_{\mathrm{W1}} = \frac{(16-\Delta^2+|\Delta|\tilde{\Delta})^{1/2}(3|\Delta|+\tilde{\Delta})\alpha B_0}{16\sqrt{2}}, \qquad (14)$$

where $\tilde{\Delta} = (\Delta^2+32)^{1/2}$. For a large E one has simply $B_{\mathrm{W}} \sim \alpha E$, and further, the Walker velocity $v_{\mathrm{W}} \sim E$. The analytical results of B_{W} and v_{W} versus E are shown as red solid lines in Figs. 3(b) and 3(c), respectively, which are both consistent with the numerical simulations.

B. Electric field induced DW chirality switching

In this section, we investigate the effect of the applied electric field on the chirality of DW. We show that a reliable control of the chirality switching of a moving DW will be achieved by the application of an electric field along the direction of the magnetic field. Each DW has two possible chiralities: CW and CCW. This DW chirality can be used as an information unit.[2] Therefore, a controllable switching of the DW chirality is desirable.

We now change the direction of the applied electric field to align the $-\hat{z}$ direction, i.e., parallel to the magnetic field. The numerical results are shown in Fig. 4. Figure 4(a) illustrates the v_{DW} (B) curves for various E. We can see that a negative E also results in a suppression of the Walker breakdown and an increase of the DW velocity, similar to the action of a positive E discussed in Sec. III. On the other hand, the chirality of the DW is determined by the tilt angle $\phi_0(t)$. It should be noted that $\phi_0(t)$ increases from the initial tilt angle ϕ_{0i} but eventually becomes saturated to a constant value in the limit $t \to \infty$ below the Walker breakdown. Hence, controlling the terminal tilt angle ϕ_0 can be used to switch the chirality of the DW. For a moving DW driven purely by a magnetic field, its initial chirality is preserved below the Walker field,[40] and the chirality switching is difficult to achieve in a controllable way. However, it can be shown that this picture will not hold for multiferroic DW when E is included. Figure 4(b) shows the terminal DW tilt angle ϕ_{DW} $(=\phi_0(t\to\infty))$ as a function of the external magnetic field B in the presence of electric field E. We can see that below the Walker field, the DW tilt angle ϕ_{DW} initially

increases with B from zero, and then suddenly jumps to a value larger than π at a critical field B_c for each E. Therefore, the switching of the DW chirality from the initially clockwise to terminally counterclockwise has clearly occurred at these critical magnetic fields. Fig. 4(c) further shows the x-component of the spin at the DW center for the applied fields B near the critical field B_c. The applied electric field is chosen as $E = -0.5E_0$. The signs of the spin component along the x-axis indicate that below B_c (i.e., $B = 0.0132B_0$), the DW chirality is CW, when B reaches up to B_c, the DW chirality switches to CCW. The positions of B_c extracted from the $\phi_{DW}(B)$ curves are shown as blue spheres in Fig. 4(d). It is shown that B_c decreases with $|E|$ down to zero at $|E| = 2E_0$.

In order to better understand this remarkable chirality switching process, we take the following analytical analyses. For a negative E, we can obtain from Eq. (13) the Walker field $B_W(\phi_{0i} = 0, E < 0) = B_{W2}$, with

$$B_{W2} = \frac{(16 - \Delta^2 - |\Delta|\tilde{\Delta})^{1/2}(-3|\Delta| + \tilde{\Delta})\alpha B_0}{16\sqrt{2}}. \quad (15)$$

For smaller negative E, we have $B_W(\phi_{0i} = 0, E < 0) \sim -\alpha E$. Interestingly, if setting the initial tilt angle $\phi_{0i} = \pi$ (i.e., the initial chirality is CCW), we can also obtain the Walker field as $B_W(\phi_{0i} = \pi, E < 0) = B_{W1}$. In this case, the terminal tilt angle ϕ_{DW} is larger than π. Moreover, it is easy to see that for $E < 0$, $B_W(\phi_{0i} = 0, E < 0)$ is smaller than $B_W(\phi_{0i} = \pi, E < 0)$. Such a difference between the two Walker fields $B_W(\phi_{0i} = 0, E < 0)$ and $B_W(\phi_{0i} = \pi, E < 0)$ enables the chirality of a moving DW to be switched. That is, when B increases beyond the first Walker field $B_W(\phi_{0i} = 0, E < 0)$, the Walker breakdown process does not occur until B further reaches the higher Walker field $B_W(\phi_{0i} = \pi, E < 0)$. In the meantime, the initial tilt angle ϕ_{0i} switches from 0 to π at the first threshold field $B_W(\phi_{0i} = 0, E < 0)$ and thus the DW chirality can be switched. The E dependence of $B_W(\phi_{0i} = 0, E < 0)$ is shown in Fig. 4(d) as red solid line, which is in excellent agreement with the numerical results B_c extracted from the $\phi_{DW}(B)$ curves. However, for $E > 0$, $B_W(\phi_{0i} = 0, E > 0) > B_W(\phi_{0i} = \pi, E > 0)$, we have only one threshold field $B_W(\phi_{0i} = 0, E > 0)$ and hence there is no DW chirality switching process. The switching of the DW chirality with the application of electric field can be read by a magnetic field sensor since the stray field near a DW depends on its chirality. It should be noted that the controlled chirality switching of a moving DW can also be achieved by applying an oblique magnetic field as proposed by Seo *et al.*[41] Nevertheless, we here offer a more efficient alternative to flip the chirality of the DW with the help of an external electric field.

IV. SUMMARY

We considered multiferroic DW systems that exhibit both a coexistence and a coupling of electric polarization and a magnetic DW. The effects of electric field on the DW dynamics via the inhomogeneous magnetoelectric interaction have been investigated. We have revealed the dynamical nature of a multiferroic DW and demonstrated the efficiency of an electric field control of magnetic DW motion. In particular, we showed that the electric field can achieve not only a nearly linear enhancement of the maximum wall velocity but also a controllable switching of DW chirality. This control of the motion of the multiferroic DWs via electric fields can be useful for designing low-power and high-speed DW-based magnetoelectric memory and logic devices.

ACKNOWLEDGMENTS

This work was supported by NSF-China (Grant Nos. 11074216 and 11274272), the Fundamental Research Funds for the Central Universities in China, and China Postdoctoral Science Foundation.

[1]G. Catalan, J. Seidel, R. Ramesh, and J. F. Scott, Rev. Mod. Phys. **84**, 119 (2012).
[2]D. A. Allwood, G. Xiong, C. C. Faulkner, D. Atkinson, D. Petit, and R. P. Cowburn, Science **309**, 1688 (2005); S. S. P. Parkin, M. Hayashi, and L. Thomas, *ibid.* **320**, 190 (2008).
[3]N. L. Schryer and L. R. Walker, J. Appl. Phys. **45**, 5406 (1974).
[4]X. R. Wang, P. Yan, and J. Lu, Europhys. Lett. **86**, 67001 (2009); B. Hu and X. R. Wang, Phys. Rev. Lett. **111**, 027205 (2013).
[5]G. S. D. Beach, C. Nistor, C. Knutson, M. Tsoi, and J. L. Erskine, Nature Mater. **4**, 741 (2005).
[6]L. Berger, J. Appl. Phys. **55**, 1954 (1984).
[7]G. Tatara and H. Kohno, Phys. Rev. Lett. **92**, 086601 (2004); S. Zhang and Z. Li, *ibid.* **93**, 127204 (2004); A. Thiaville, Y. Nakatani, J. Miltat, and Y. Suzuki, Europhys. Lett. **69**, 990 (2005).
[8]M. T. Bryan, T. Schrefl, D. Atkinson, and D. A. Allwood, J. Appl. Phys. **103**, 073906 (2008).
[9]S. Glathe, I. Berkov, T. Mikolajick, and R. Mattheis, Appl. Phys. Lett. **93**, 162505 (2008).
[10]A. Kunz and S. C. Reiff, J. Appl. Phys. **103**, 07D903 (2008).
[11]K. Richter, R. Varga, G. A. Badini-Confalonieri, and M. Vázquez, Appl. Phys. Lett. **96**, 182507 (2010).
[12]J.-Y. Lee, K.-S. Lee, and S.-K. Kim, Appl. Phys. Lett. **91**, 122513 (2007).
[13]S.-W. Jung, W. Kim, T.-D. Lee, K.-J. Lee, and H.-W. Lee, Appl. Phys. Lett. **92**, 202508 (2008).
[14]S. Emori and G. S. D. Beach, Appl. Phys. Lett. **98**, 132508 (2011).
[15]K. Obata and G. Tatara, Phys. Rev. B **77**, 214429 (2008).
[16]O. A. Tretiakov and A. Abanov, Phys. Rev. Lett. **105**, 157201 (2010); A. Thiaville, S. Rohart, E. Jue, V. Cros, and A. Fert, Europhys. Lett. **100**, 57002 (2012).
[17]K.-W. Kim, S.-M. Seo, J. Ryu, K.-J. Lee, and H.-W. Lee, Phys. Rev. B **85**, 180404(R) (2012); J. Ryu, K.-J. Lee, and H.-W. Lee, Appl. Phys. Lett. **102**, 172404 (2013).
[18]K. S. Ryu, L. Thomas, S. H. Yang, and S. S. P. Parkin, Nat. Nanotechnol. **8**, 527 (2013).
[19]S. Emori, U. Bauer, S. M. Ahn, E. Martinez, and G. S. D. Beach, Nature Mater. **12**, 611 (2013).
[20]M. Weisheit, S. Fahler, A. Marty, Y. Souche, C. Poinsignon, and D. Givord, Science **315**, 349 (2007).
[21]M. Endo, S. Kanai, S. Ikeda, F. Matsukura, and H. Ohno, Appl. Phys. Lett. **96**, 212503 (2010).
[22]U. Bauer, S. Emori, and G. S. D. Beach, Appl. Phys. Lett. **100**, 192408 (2012).
[23]A. J. Schellekens, A. van den Brink, J. H. Franken, H. J. M. Swagten, and B. Koopmans, Nat. Commun. **3**, 847 (2012).
[24]D. Chiba, M. Kawaguchi, S. Fukami, N. Ishiwata, K. Shimamura, K. Kobayashi, and T. Ono, Nat. Commun. **3**, 888 (2012).
[25]U. Bauer, S. Emori, and G. S. D. Beach, Appl. Phys. Lett. **101**, 172403 (2012).
[26]A. Bernand-Mantel, L. Herrera-Diez, L. Ranno, S. Pizzini, J. Vogel, D. Givord, S. Auffret, O. Boulle, I. M. Miron, and G. Gaudin, Appl. Phys. Lett. **102**, 122406 (2013).
[27]J. H. Franken, Y. Yin, A. J. Schellekens, A. van den Brink, H. J. M. Swagten, and B. Koopmans, Appl. Phys. Lett. **103**, 102411 (2013).
[28]U. Bauer, S. Emori, and G. S. D. Beach, Nat. Nanotechnol. **8**, 411 (2013).
[29]S.-W. Cheong and M. Mostovoy, Nature Mater. **6**, 13 (2007).

[30]H. Katsura, N. Nagaosa, and A. V. Balatsky, Phys. Rev. Lett. **95**, 057205 (2005).
[31]C. Jia, S. Onoda, N. Nagaosa, and J. H. Han, Phys. Rev. B **74**, 224444 (2006); **76**, 144424 (2007).
[32]H. B. Chen, Y. Zhou, and Y. Q. Li, J. Phys.: Condens. Matter **25**, 286004 (2013).
[33]H. B. Chen and Y. Q. Li, Appl. Phys. Lett. **102**, 252906 (2013).
[34]M. Mostovoy, Phys. Rev. Lett. **96**, 067601 (2006).
[35]V. G. Bar'yakhtar, V. A. Lvov, and D. A. Yablonskii, JETP Lett. **37**, 673 (1983).
[36]A. S. Logginov, G. A. Meshkov, A. V. Nikolaev, E. P. Nikolaeva, A. P. Pyatakov, and A. K. Zvezdin, Appl. Phys. Lett. **93**, 182510 (2008).
[37]A. P. Pyatakov, D. A. Sechin, A. S. Sergeev, A. V. Nikolaev, E. P. Nikolaeva, A. S. Logginov, and A. K. Zvezdin, Europhys. Lett. **93**, 17001 (2011).
[38]I. E. Dzyaloshinskii, Europhys. Lett. **83**, 67001 (2008).
[39]D. L. Mills and I. E. Dzyaloshinskii, Phys. Rev. B **78**, 184422 (2008).
[40]G. Tatara, H. Kohno, and J. Shibata, Phys. Rep. **468**, 213 (2008).
[41]S.-M. Seo, K.-J. Lee, S.-W. Jung, and H.-W. Lee, Appl. Phys. Lett. **97**, 032507 (2010).